

10  
12/10/90

K.M.R.

(1)

# SPIN PHYSICS WITH POLARIZED ELECTRONS AT THE SLC\*

Kenneth C. Moffeit  
Stanford Linear Accelerator Center,  
Stanford University, Stanford, CA 94309, USA

## Abstract

The Stanford Linear Collider was designed to accommodate polarized electron beams. A gallium arsenide-based photon emission source will provide a beam of longitudinally polarized electrons of about 40 percent polarization. A system of bend magnets and a superconducting solenoid will be used to rotate the spins so that the polarization is preserved while the 1.21 GeV electrons are stored in the damping ring. Another set of bend magnets and two superconducting solenoids orient the spin vectors so that longitudinal polarization of the electrons is achieved at the collision point with the unpolarized positrons. A system to monitor the polarization based on Møller and Compton scattering will be used.

Spin physics with longitudinally polarized electrons uses the measurement of the left-right asymmetry to provide tests of the Standard Model. The uncertainty in the measurement is precise enough to be sensitive to the effects of particles which can not be produced directly in the machines we have today.

## 1. INTRODUCTION

The Stanford Linear Collider (SLC) at the Stanford Linear Accelerator Center is unique among existing or planned colliding beam facilities in its potential to accelerate longitudinally polarized electrons. The polarization sense is reversible from pulse to pulse at the operator's control, and thereby precise tests of the coupling of fermions through the measurement of the left-right asymmetry

$$A_{LR} = \frac{\sigma_L - \sigma_R}{\sigma_L + \sigma_R} \tag{1}$$

can be made. Here  $\sigma_L(\sigma_R)$  is the cross section for left-handed (right-handed) electrons

\* Work supported by Department of Energy contract DE-AC03-76SF00515.

*Invited talk presented at the 9th International Symposium on High Energy Spin Physics, Bonn, West Germany, September 10-15, 1990.*

MASTER 

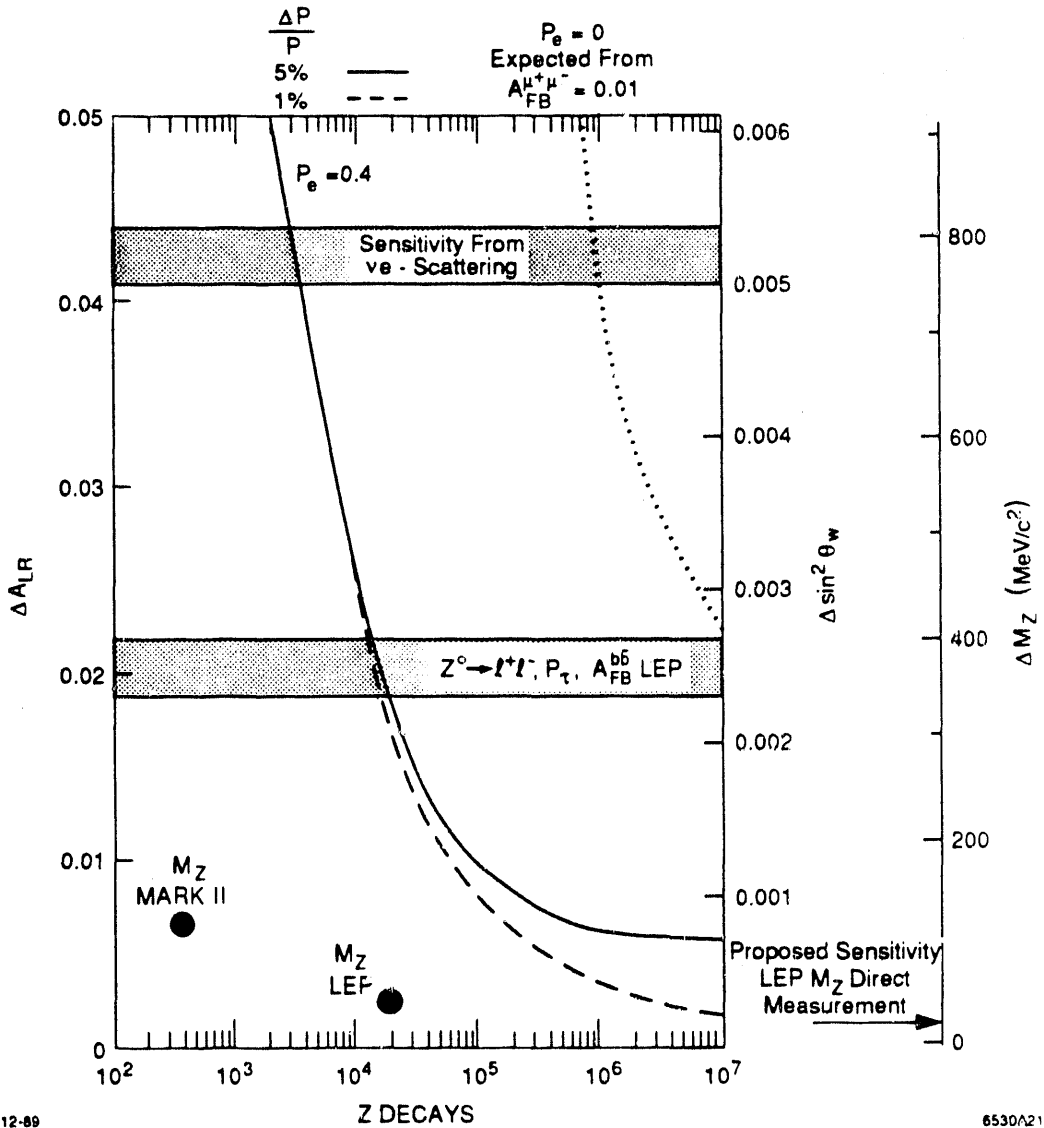


**Figure 1:** The expected uncertainty of a measurement of the left-right asymmetry  $A_{LR}$  as a function of the number of  $Z^0$  events accumulated. The beam polarization is taken to be 40%. The  $Z^0$  mass is assumed to be 91.17 GeV. The corresponding uncertainty on  $\sin^2\theta_W$  and on  $M_Z$  is shown on the right-hand scales. The two branches of the  $A_{LR}$  curve refer to the precision of the polarization monitoring. The expected uncertainty on  $\sin^2\theta_W$  from a measurement of the leptonic forward-backward asymmetry is also shown. The shaded regions indicate present accuracy from  $\nu$ -scattering and recent results from measurement of the leptonic branching ratio, forward-backward asymmetry and tau polarization at LEP. The direct measurement of  $M_Z$  at SLC and LEP are of sufficient accuracy to precisely calculate  $A_{LR}$  within the Standard Model.

on unpolarized positrons. In the Standard Model,  $A_{LR}$  is uniquely predicted once  $M_Z$  is known, and is independent of the final fermion type. Thus, all visible  $Z^0$  decays can be used for the precision test of the Standard Model.  $A_{LR}$  is large and has a value around 0.13 for  $M_Z = 91.17$  GeV.

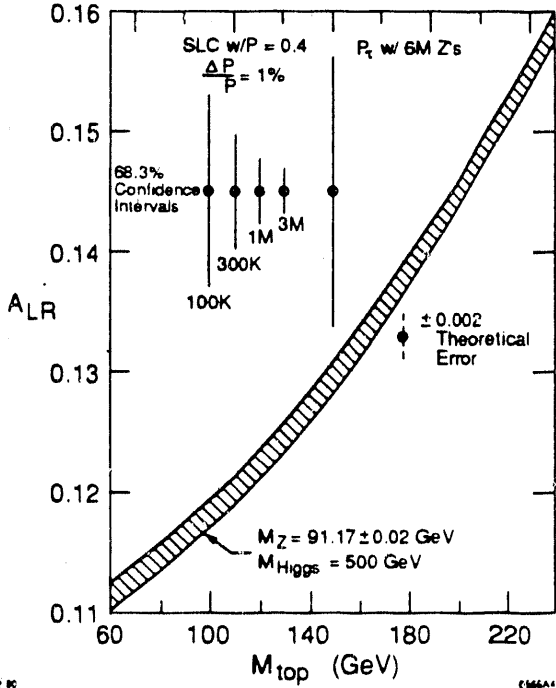


**Figure 2:** The left-right asymmetry as a function of the top quark mass. The Higgs boson mass is assumed to be 500 GeV and the  $Z^0$ -mass is taken to be  $(91.17 \pm 0.02)$  GeV. Figure taken from Reference 1.

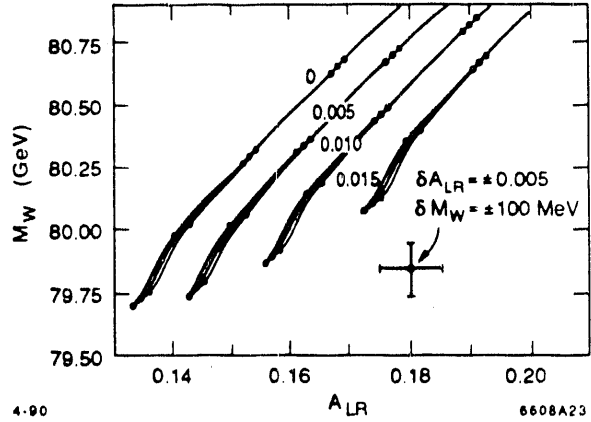
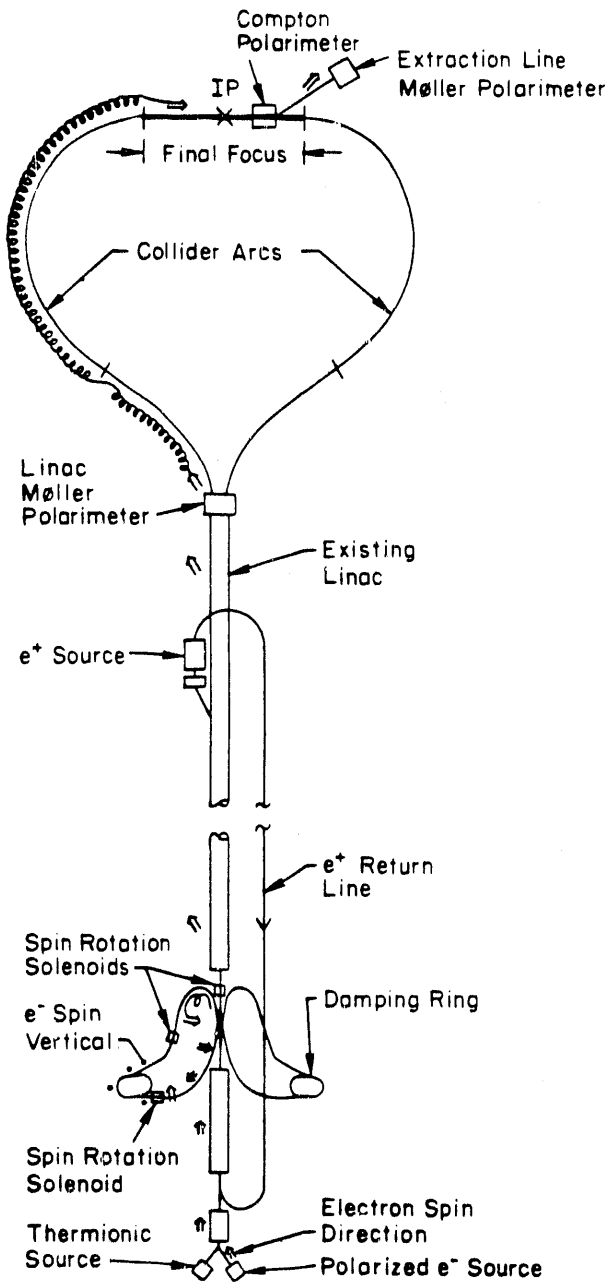


**Figure 3:** The expected values of  $M_W$  and  $A_{LR}$  are shown as  $m_{top}$  is varied from 50 GeV to 200 GeV ( $m_{Higgs}$  is fixed to 100 GeV) for the case that the Standard Model is extended to include a  $\chi$ -type  $Z'$  boson. The mass of the  $Z'$  boson is assumed to be 500 GeV. The three contours in each group correspond to the three values of the  $Z^0$  mass,  $M_Z = 91.17 \pm 0.02$  GeV. The dots along each contour indicate the points ( $m_{top} = 50, 100, 150, 200$  GeV). The four groups of contours show four values of the  $Z^0 - Z'$  mixing parameter,  $\sin\theta_m = 0.00$  (no mixing),  $-0.005$ ,  $-0.01$ ,  $-0.015$ . The precision expected from a 300 K event measurement of  $A_{LR}$  and a 100 MeV measurement of  $M_W$  is shown by the error bars in the corner of the plot. Figure taken from Reference 1.

The accuracy of the measurement of  $A_{LR}$  depends on the uncertainty in the polarization measurement and statistics. The precision anticipated at the SLC is displayed in Figure 1 as a function of the number,  $N$ , of observed  $Z$  decays. The curves correspond to different levels of precision when measuring the electron polarization. The scales on the right show the resulting precision of the  $A_{LR}$  measurement to those of  $\sin^2\theta_W$  and  $M_Z$ .

The left-right asymmetry has a number of other properties that make its precise measurement attractive.<sup>1</sup> It depends upon the  $Z^0$ -electron coupling alone and therefore is independent of final state mass effects and QCD corrections. The left-right asymmetry varies little over the  $Z^0$ -width and therefore is insensitive to initial-state QED radiation. It is also very sensitive to the electroweak mixing parameter and to virtual electroweak corrections in the presence of new particles.

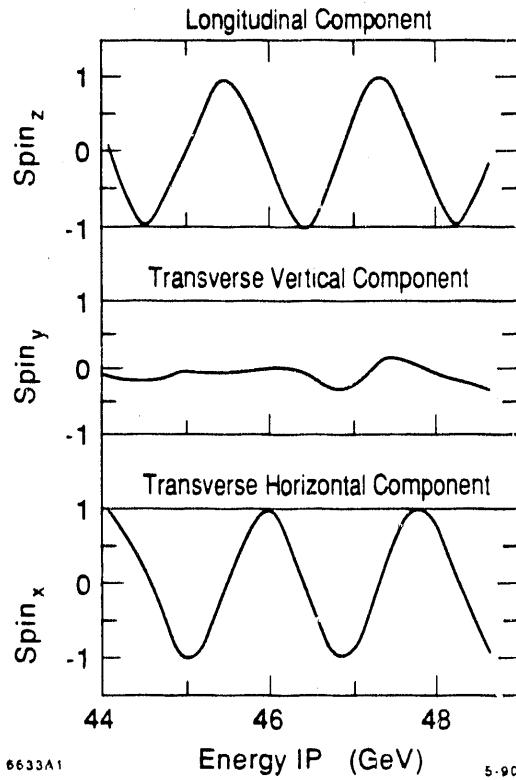


**POLARIZATION IN THE OVERALL SLC LAYOUT**

10-86

5571A4

**Figure 4:** A layout of the SLAC Linear Collider emphasizing polarization. The orientation of an electron spin vector is shown as the electron is transported from the polarized electron source to the interaction point.



6633A1

5-90

**Figure 5:** The spin vector direction at the end of the linac to give longitudinal polarization at the collision point.

For example, the theoretical expectation for  $A_{LR}$  is shown in Figure 2 for the mass of the top between 60 and 240 GeV. The accuracy of  $A_{LR}$  is shown for different numbers of  $Z^0$  in the experiment. A measurement of 300 K  $Z^0$  events constrains the top quark mass to  $\delta M_{TOP} = \pm 17$  GeV which is comparable to a 100 MeV determination of  $M_W$ .

New physical processes have different higher order corrections to different measurables. The correlation between  $M_W$  and  $A_{LR}$  is shown in Figure 3. The curves show the change in  $A_{LR}$  and  $M_W$  as  $M_{TOP}$  is varied from 50 GeV to 200 GeV. The three contours in each group correspond to  $M_Z = 90.15, 91.17$  and  $91.19$ . The other groups represent a different value of the  $Z^0 - Z'$  mixing parameter where the Standard Model is extended to include a 500 GeV,  $\chi$ -type  $Z'$  boson.<sup>1</sup> Precision measurements of both  $A_{LR}$  and  $M_W$  can distinguish between new physical processes.

## 2. OVERVIEW

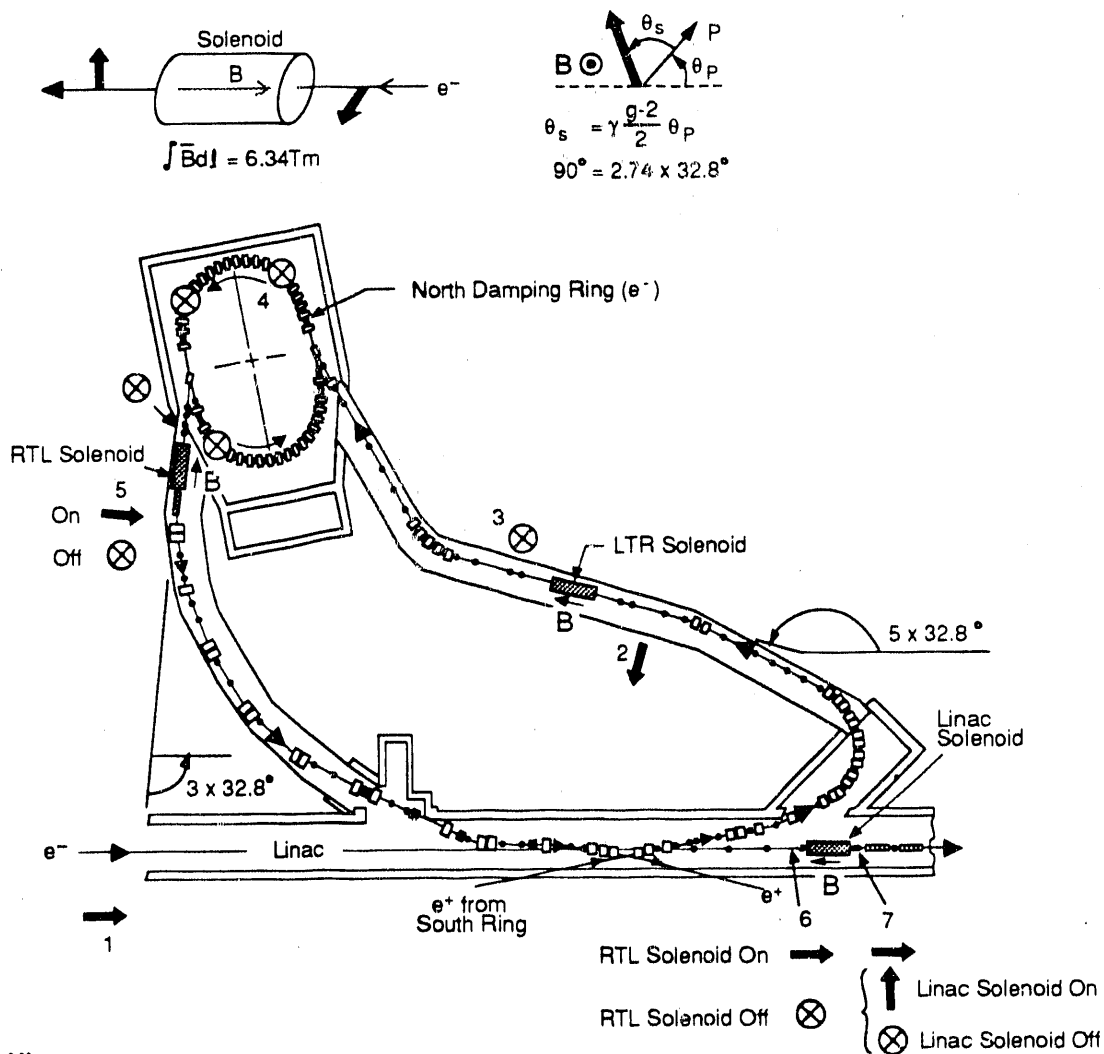
The SLC has the capability of accelerating polarized electrons and transporting these through the damping ring to the interaction region with small depolarization of the beam. A collaboration of physicists from Indiana, LBL, SLAC, and Wisconsin is preparing the systems for the polarization capability at the SLC.<sup>2</sup>

The layout of the polarized SLC is shown in Figure 4. The electrons are produced longitudinally polarized by irradiating a GaAs crystal with circularly polarized light. The source will be capable of producing beams of the required intensity and pulse structure for SLC so no degradation of luminosity is expected. Polarization of about 40% is expected with this source. Details of the SLC polarized electron source can be found in Reference 3.

To preserve the polarization while the electrons are in the damping ring, the spin direction must be transverse to the plane of the damping ring. In addition, the spin direction must be re-established after leaving the damping ring so that it points in the desired direction for acceleration to the end of the linac and transportation around the electron arc to the interaction point where longitudinal polarization is required (see Figure 5). A vertical spin component is required at some energies because of the terrain following of the arcs. Three spin-rotating solenoids of 6.34 T-m each are needed to rotate the spin. These superconducting solenoids are located at positions in the transfer lines to and from the damping ring where the spin direction has precessed  $90^\circ$  by the guide field (see Figure 6). Two of these are installed and operational and allow acceleration of transversely polarized electrons.

Two types of polarimeters based on Compton and Møller scattering will provide reliable and accurate polarization measurements near the interaction point (see Figure 7). A third Møller polarimeter at the end of the linac will serve as a useful diagnostic tool in tuning the polarization and in defining the initial spin vector. Both Møller polarimeters are capable of measuring all three components of the polarization vector.

The Møller polarimeters are well suited for use at the end of the linac and in the extraction line before the beam dump. The advantages are that the technique has been demonstrated in previous experiments with polarized beams at SLAC<sup>4</sup> and



8-88  
6104A2

**Figure 6:** The spin rotation system for the north damping ring. The orientation of the electron spin vector is shown by the full arrow.

it gives three-axis polarimetry. While the counting rate (50 to 100 Møller scatters detected per electron pulse) and the asymmetry (longitudinal asymmetry is 0.78 at  $90^\circ$  in the center of mass) are large the target polarization is only about 8%. This means that the measured asymmetry is only about 2% when the beam has polarization of 0.4. Longitudinal polarization of the beam can be measured to an accuracy of  $\Delta P/P = \pm 5\%$  in one or two minutes while transverse polarization will require about 1 hour to reach the same accuracy due to a lower asymmetry of  $1/7$  than that for longitudinal spins.

The targets, collimators and detectors for the Møller polarimeters are installed. In Figure 8 the Møller peak can be seen above background in the data from the linac Møller polarimeter. While improvements to the linac polarimeter are in progress this polarimeter is operational and available for spin dynamic studies.

A polarimeter making use of the Compton effect can be used to measure the absolute electron polarization to about 2% accuracy, and to monitor rapidly relative changes

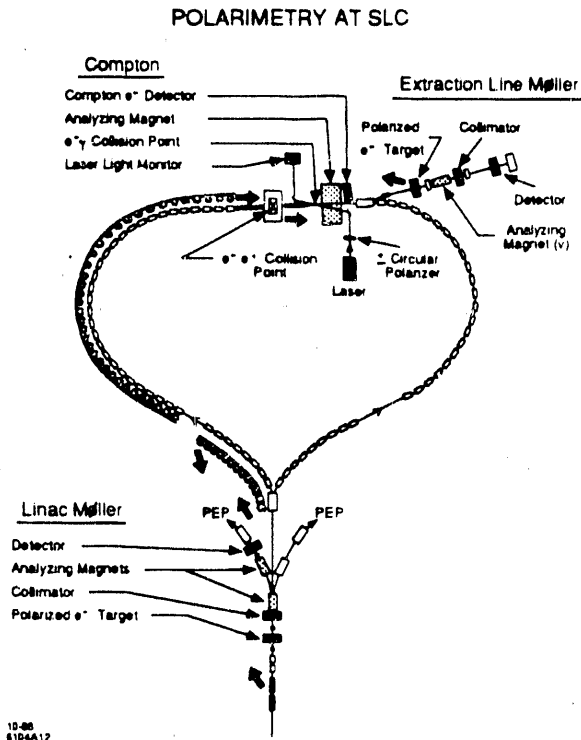


**Figure 7:** Location of the polarimeters at the SLC. The elements of the polarimeters based on Möller and Compton scattering are indicated.

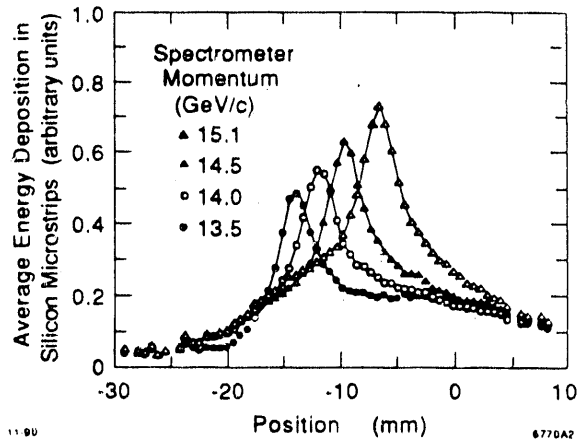


**Figure 8:** These data were taken with four different settings of the spectrometer central momentum (13.5 → 15.1 GeV/c.) The detector acceptance was  $\Delta P/P \approx 8\%$ . The expected scattering angle momentum dependence for  $ee$  scattering predicts  $\Delta y \sim 4.3 \text{ mm} * \Delta P \text{ (GeV)}$  at the Möller detector.

in polarization during operation. Such a polarimeter is being prepared to monitor the electron polarization near the IP (see Figure 9). A circularly polarized laser beam intercepts the electron beam 107 feet downstream of the interaction point. Recoiling electrons at the maximum Compton angle emerge directly forward in the laboratory with momentum less than half that of the beam, from which they are separated in the field of the soft and hard bend magnets as they head toward the electron dump. The asymmetry of the reaction rate, when either photon or electron polarization is reversed, can be 75% or higher for backward Compton scattering. The counting rates are high. The known backgrounds are expected to be tolerable and can be explicitly subtracted by using spills when the laser is not pulsed. A sufficient number of counts to achieve 2% statistical accuracy can be accumulated in a few tens of seconds. The SLC Compton Polarimeter can only measure the longitudinal component of the beam spin vector.

The systems of the Compton polarimeter are installed and commissioning studies are in progress. Compton scattered electrons were first observed in January 1990. The pulse height distribution from the Čerenkov detector is shown in Figure 10. A clear Compton signal is observed with the laser light on. Measurements of the average electron polarization are now possible with an accuracy of  $\Delta P/P < 10\%$ . Upgrades to the optics line and detector are in progress to reduce this error to a few percent.

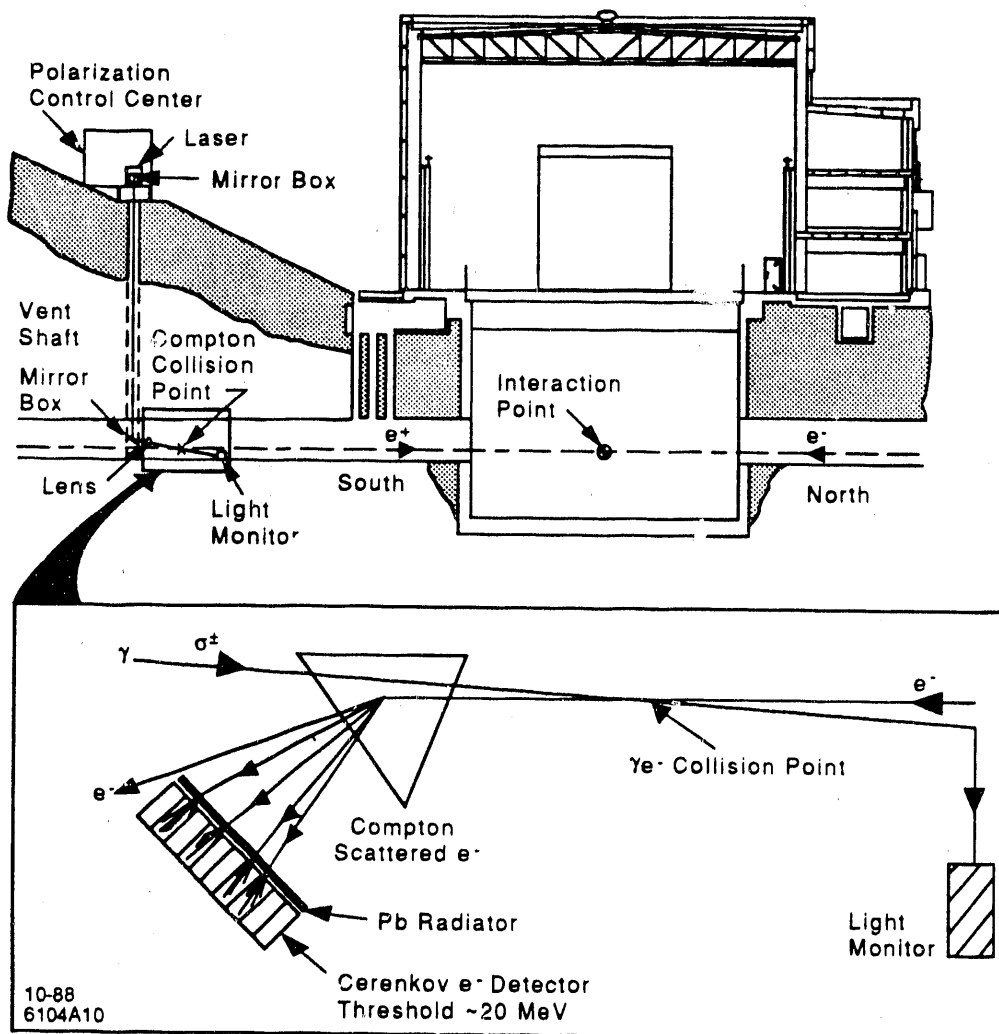
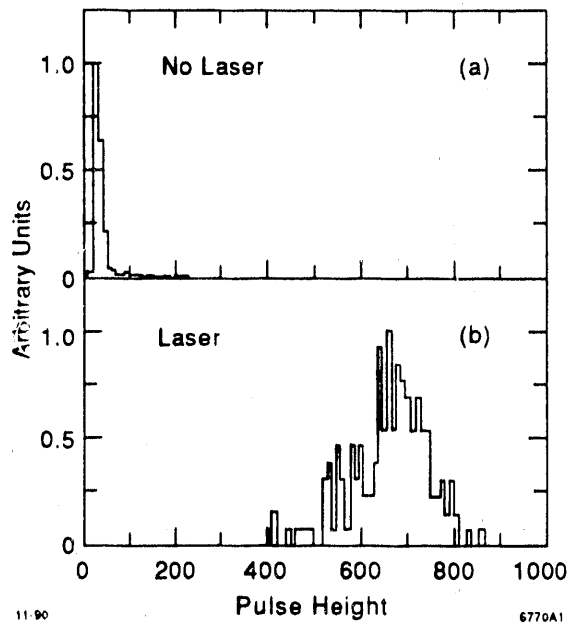


Figure 9: Location of the SLC Compton polarimeter components is shown. The light from the laser on the surface is directed into collision with the electron beam after it has passed through the interaction point.

### 3. DEPOLARIZATION EFFECTS

Depolarization of the beam can occur during the acceleration and transport of the beam to the interaction region. Most of the depolarization effects are small such as those during acceleration and in the damping ring when depolarizing resonances are avoided. However, there are two effects which cause moderate depolarization. The first of these is due to the damping ring running at 1.153 GeV instead of the value of 1.21 GeV. As a result, the spin precession in the linac-to-ring is smaller and the spin vector is not quite perpendicular to the beam direction as the beam enters the LTR solenoid. Until the ring can operate at 1.21 GeV, a  $0.069 \cdot P$  depolarization will occur. The other significant depolarization effect is caused by the finite energy spread ( $\Delta E/E = \pm 0.3\%$ ) of the beam; the energy dependence in the spin precession gives a spread in the spin





**Figure 10:** Pulse height distribution from the Čerenkov detector in the Compton Polarimeter: (a) no laser light; (b) laser light colliding with electron beam.

vector at the end of the arc resulting in a  $0.05 \cdot P$  depolarization effect.

There can also be depolarization from the beam-beam collisions and the final focus system element, but with SLC parameters, these effects are negligible.

#### 4. DETECTORS AT THE SLC

The SLD detector<sup>5</sup> has charged particle tracking and photon detection over nearly  $4\pi$  solid angle. It also has good hadron calorimetry and full particle identification. The polarization sign and the average longitudinal polarization will be recorded with each  $Z^0$  and luminosity event. The left-right asymmetry can then be determined from the analysis of these data. The demands on the detector from the point of view of the left-right asymmetry measurement is minimal, namely, the acceptance must be forward-backward symmetric.

#### REFERENCES

1. M. Swartz, SLAC-PUB-5219.
2. D. Blockus et al., Proposal for Polarization at SLC, SLAC-PROPOSAL-SLC-01 (1986).
3. J. Clendenin, "The SLC Polarized Electron Source," Proceedings of the 9th International Symposium on High Energy Spin Physics.
4. C. Y. Prescott et al., Physics Letters B77, 347 (1978).
5. SLD Design Report, SLAC-Report-273.

### **DISCLAIMER**

This report was prepared as an account of work sponsored by an agency of the United States Government. Neither the United States Government nor any agency thereof, nor any of their employees, makes any warranty, express or implied, or assumes any legal liability or responsibility for the accuracy, completeness, or usefulness of any information, apparatus, product, or process disclosed, or represents that its use would not infringe privately owned rights. Reference herein to any specific commercial product, process, or service by trade name, trademark, manufacturer, or otherwise does not necessarily constitute or imply its endorsement, recommendation, or favoring by the United States Government or any agency thereof. The views and opinions of authors expressed herein do not necessarily state or reflect those of the United States Government or any agency thereof.

**END**

**DATE FILMED**

12 / 28 / 90

